# Supplementary Information

Overcoming $BRAF^{V600E}$ Acquired Resistance in Melanoma by Deciphering and Targeting Personalized Protein Network Alterations

S. Vasudevan[#], E. Flashner-Abramson[#], Heba Alkhatib, Sangita Roy Chowdhury, I. Adesoji Adejumobi, D. Vilencki, S. Stefansky, A.M. Rubinstein and N. Kravchenko-Balasha*

The Institute of Biomedical and Oral Research, Hebrew University of Jerusalem, Jerusalem 91120, Israel

*Corresponding author: natalyk@ekmd.huji.ac.il

# Equal contribution

**Table of contents:**

## Contents

Supplementary Figure 1. ..... 2

Supplementary Figure 2. ..... 5

Supplementary Figure 3. ..... 6

Supplementary Figure 4. ..... 9

Supplementary Figure 5. ..... 10

Supplementary Figure 6. ..... 13

Supplementary Figure 7. ..... 14

Supplementary Data Legends ..... 15

Original Western Blots ..... 16

Supplementary References ..... 23

## Supplementary Figures

## Supplementary Figure 1.

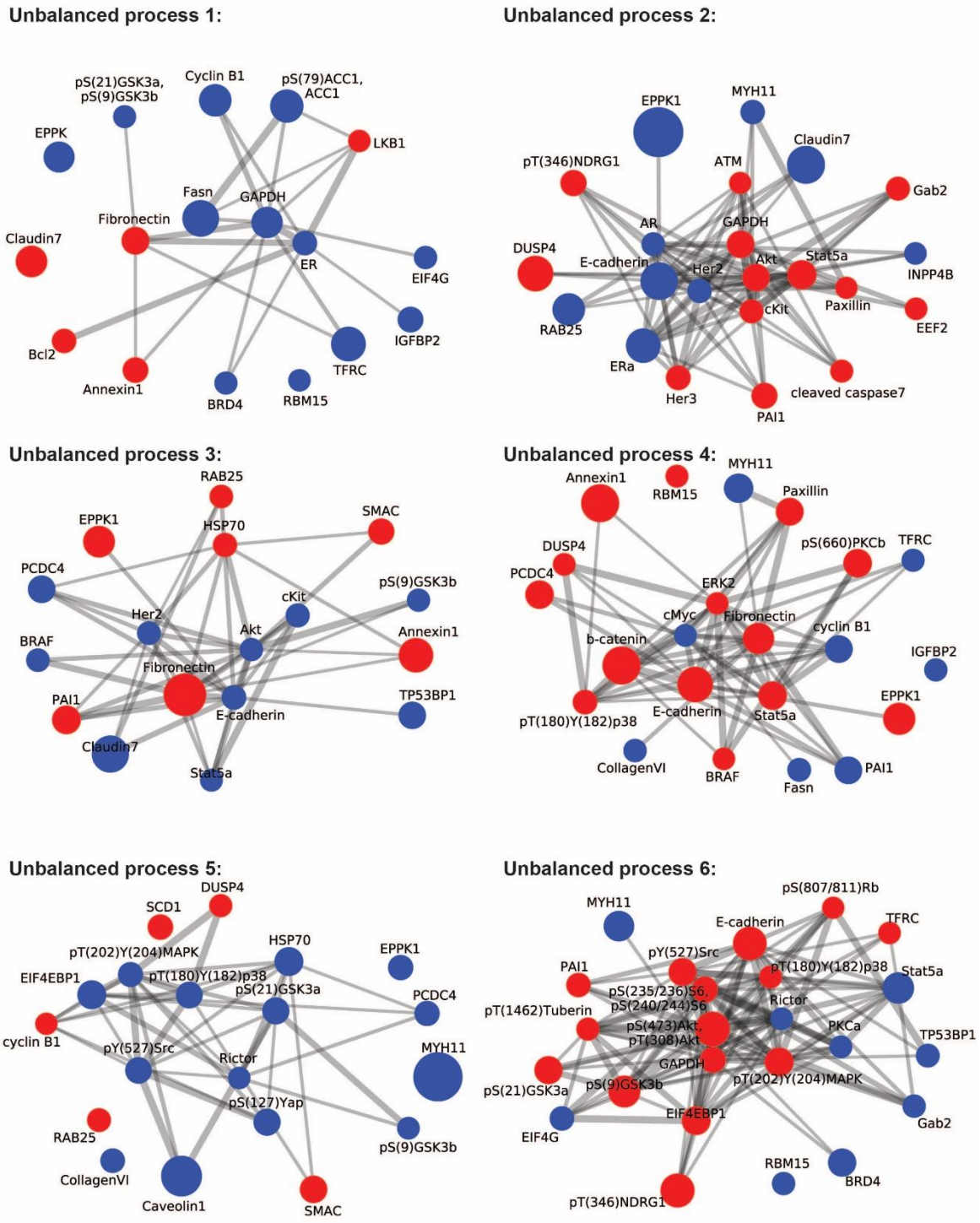

**Unbalanced process 7:**

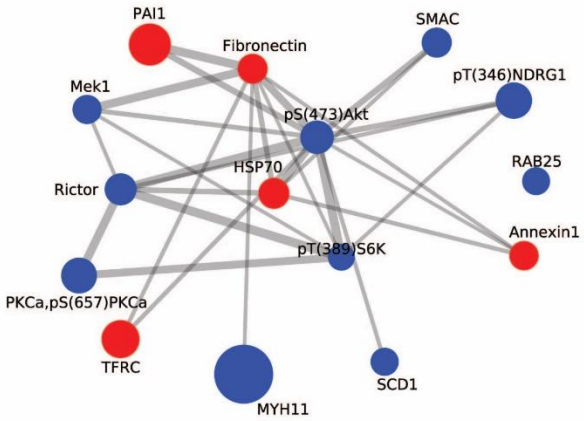


**Unbalanced process 8:**

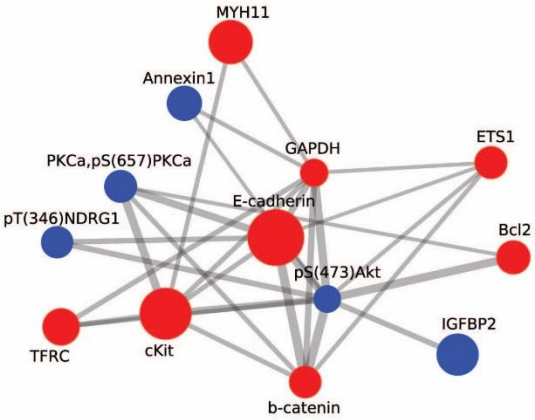


**Unbalanced process 9:**

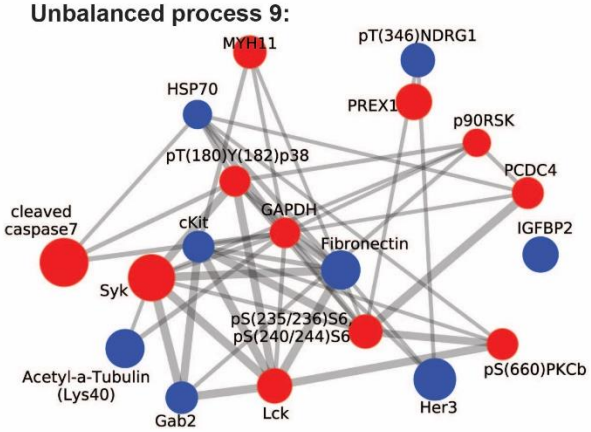


**Unbalanced process 10:**

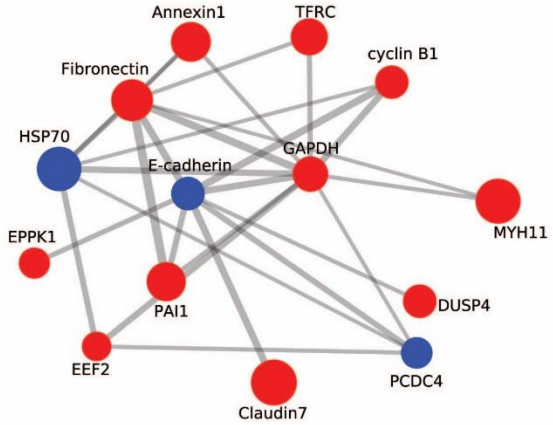


**Unbalanced process 11:**

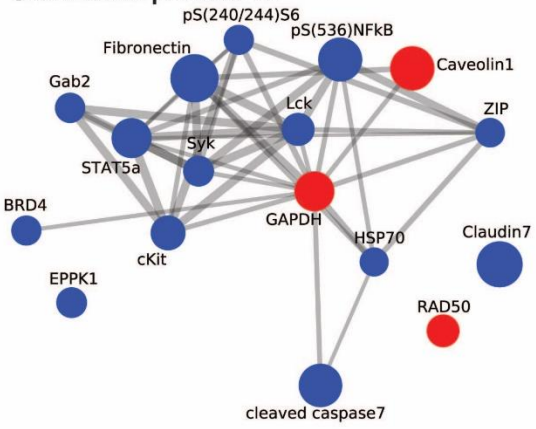


**Unbalanced process 12:**

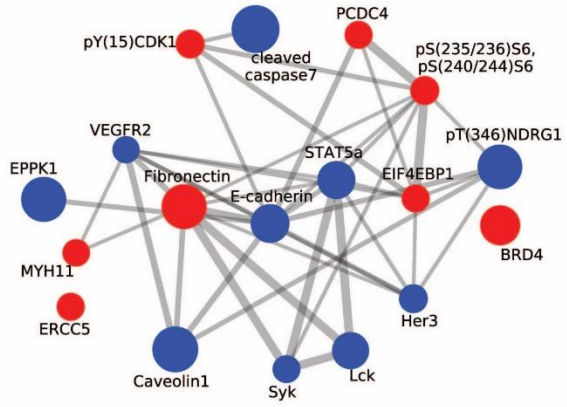

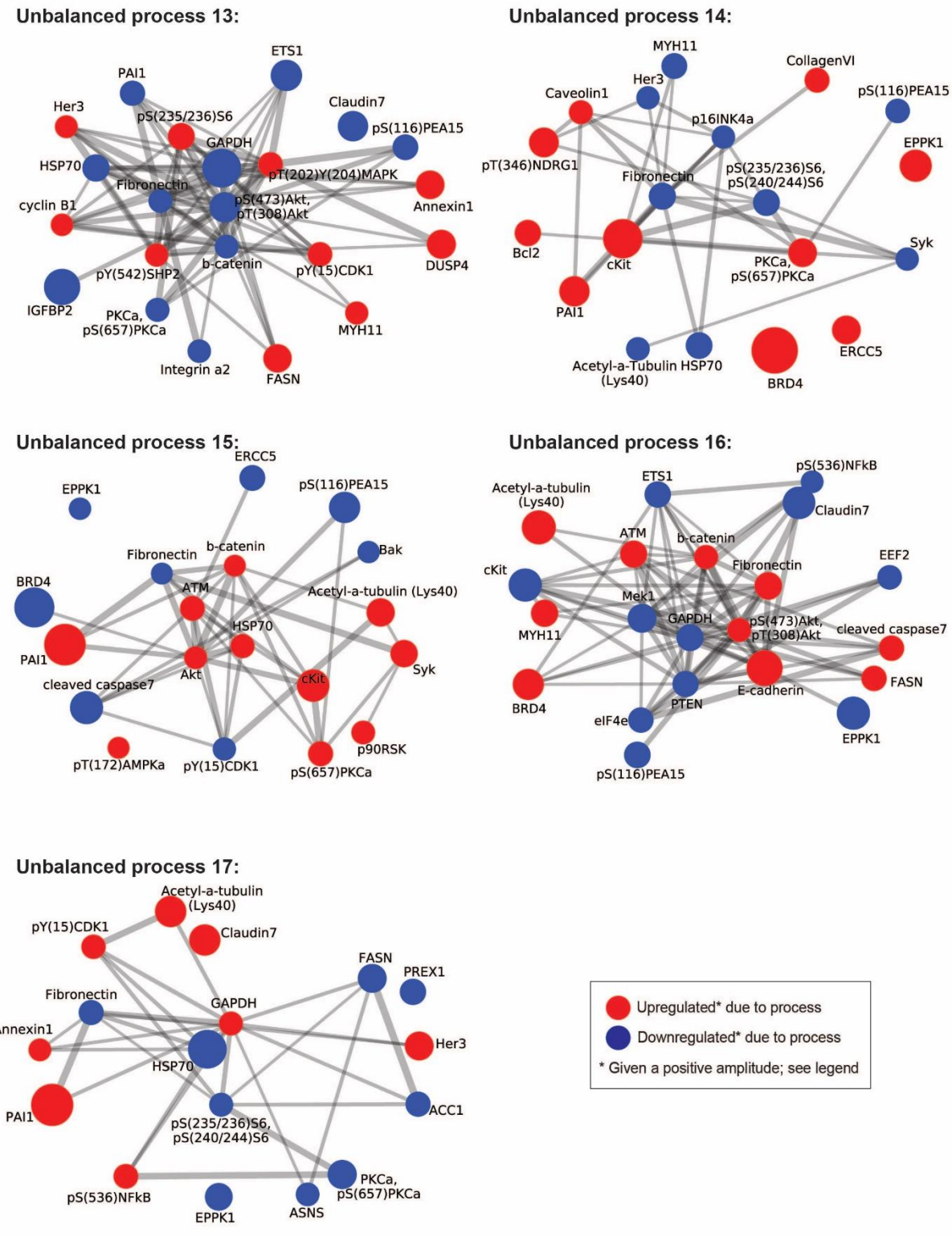


**Supplementary Figure 1. The unbalanced subnetworks identified by PaSSS analysis for 725 SKCM and THCA tumors.** For every process α, the proteins were assembled into networks using functional interactions according to STRING database. **Note** that red proteins are upregulated, and blue proteins are downregulated given that the amplitude of the process is positive. In tumors where the amplitude is negative, the direction of change is opposite.

**Supplementary Figure 2.**

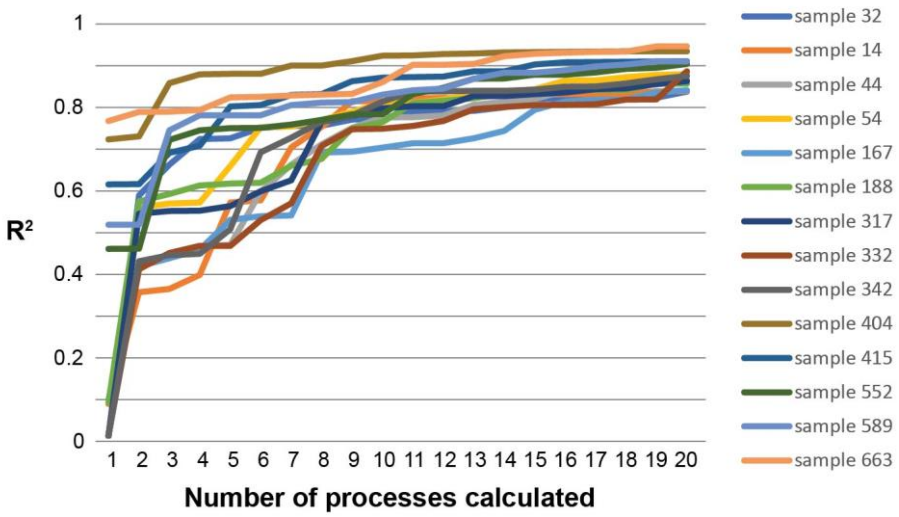


**Supplementary Figure 2. 17 unbalanced processes suffice to describe the biological imbalance in 725 tumors.** Presented are $R^2$ values for 14 random patients. The $R^2$ was calculated for every patient by plotting the natural logarithm of the experimental data (LnXi) vs. $\sum G_{i\alpha}\lambda_{\alpha}(k)$ for $\alpha = 0,1,2,....,20$. As more constraints are added, we expect to get higher agreement between the experimental data and the theoretical calculation, reaching the highest level of correlation when the experimental data is fully reproduced by the theoretical fitting. The plot reaches a plateau after the 17$^{th}$ constraint. This indicates that for $\alpha = 18,19,20...$ the data includes mainly noise.

**Supplementary Figure 3.**

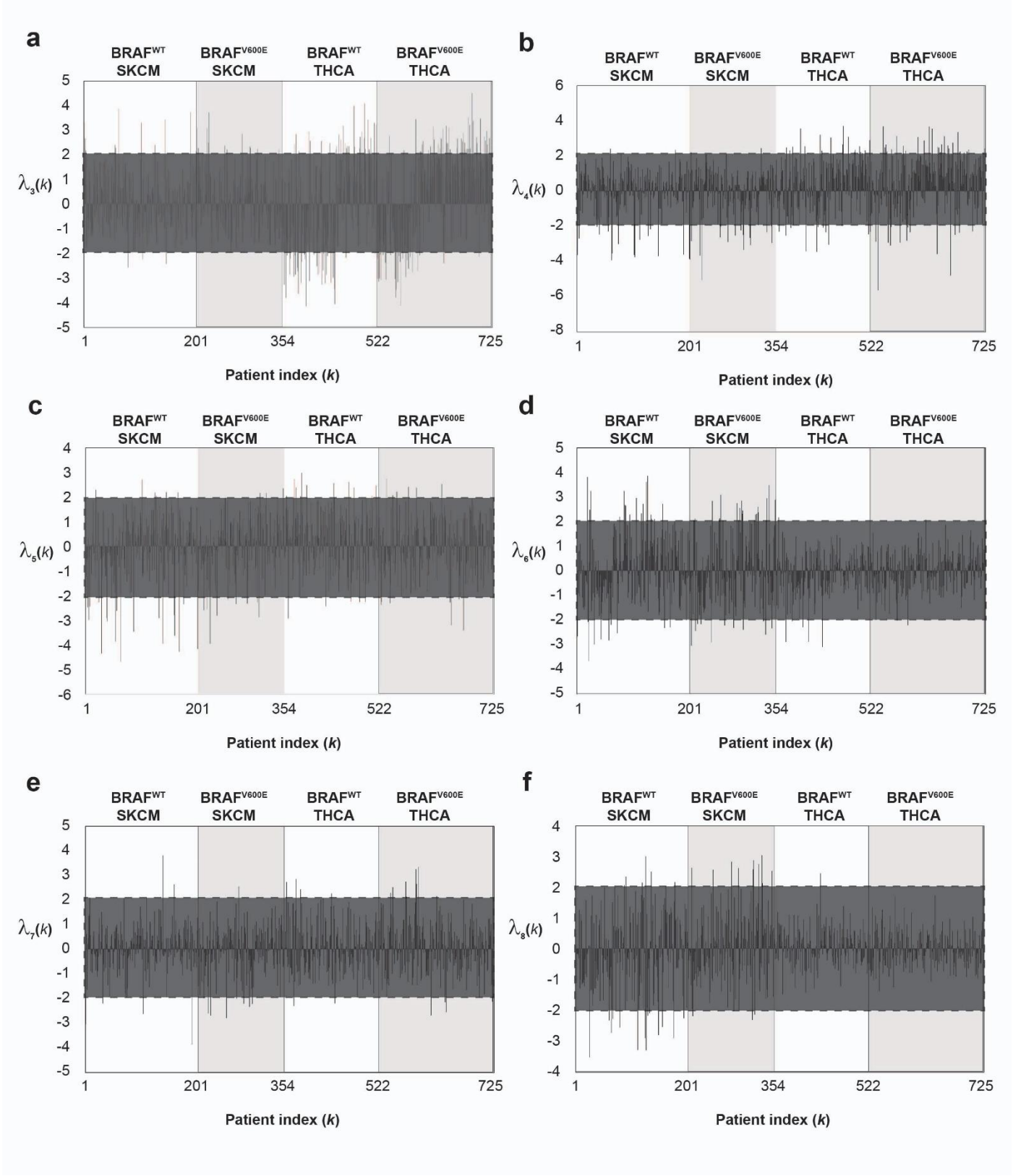

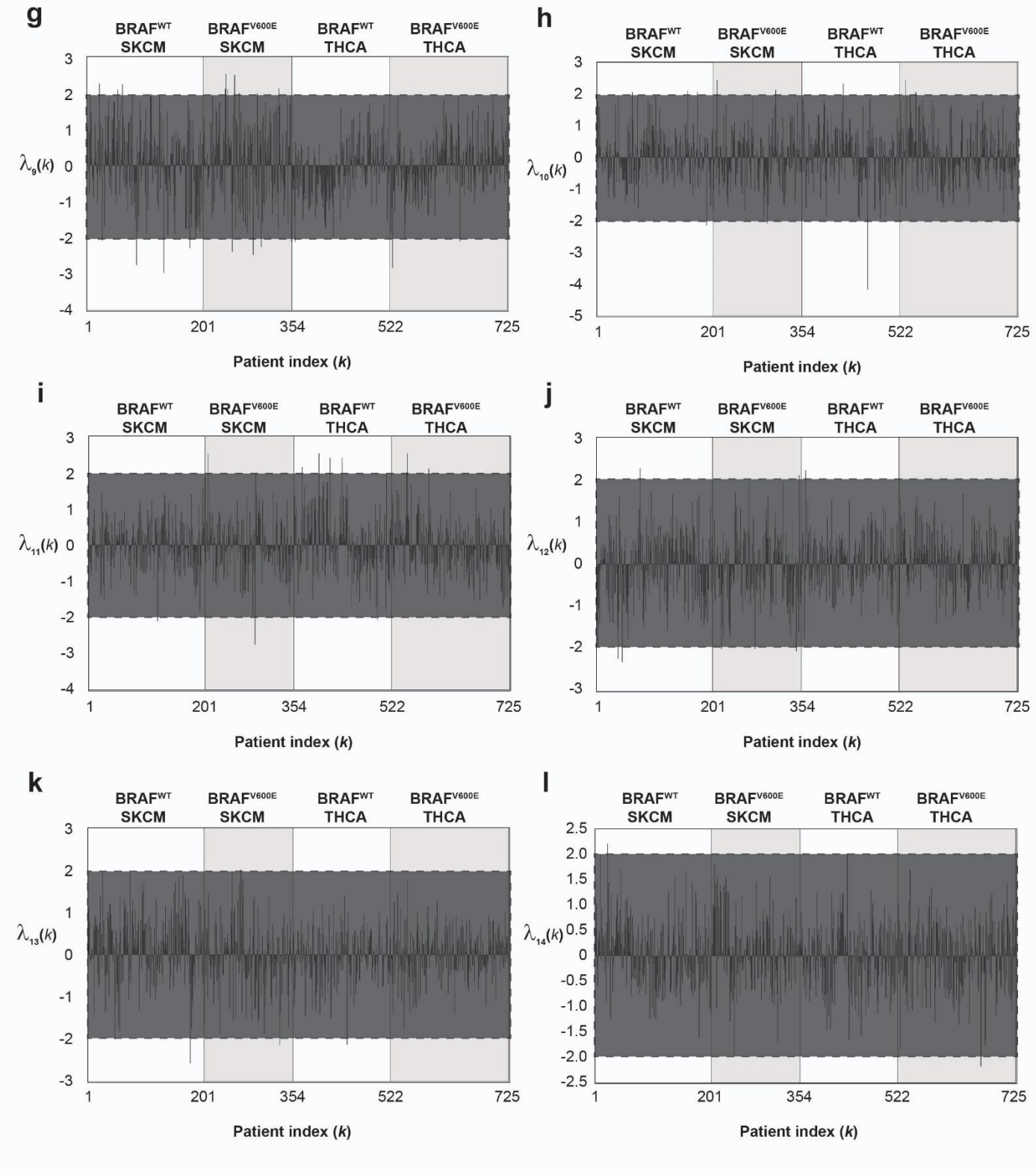
g
h
i
j
k
l
BRAF^WT SKCM
BRAF^V600E SKCM
BRAF^WT THCA
BRAF^V600E THCA
λ9(k)
λ10(k)
λ11(k)
λ12(k)
λ13(k)
λ14(k)
Patient index (k)
1
201
354
522
725

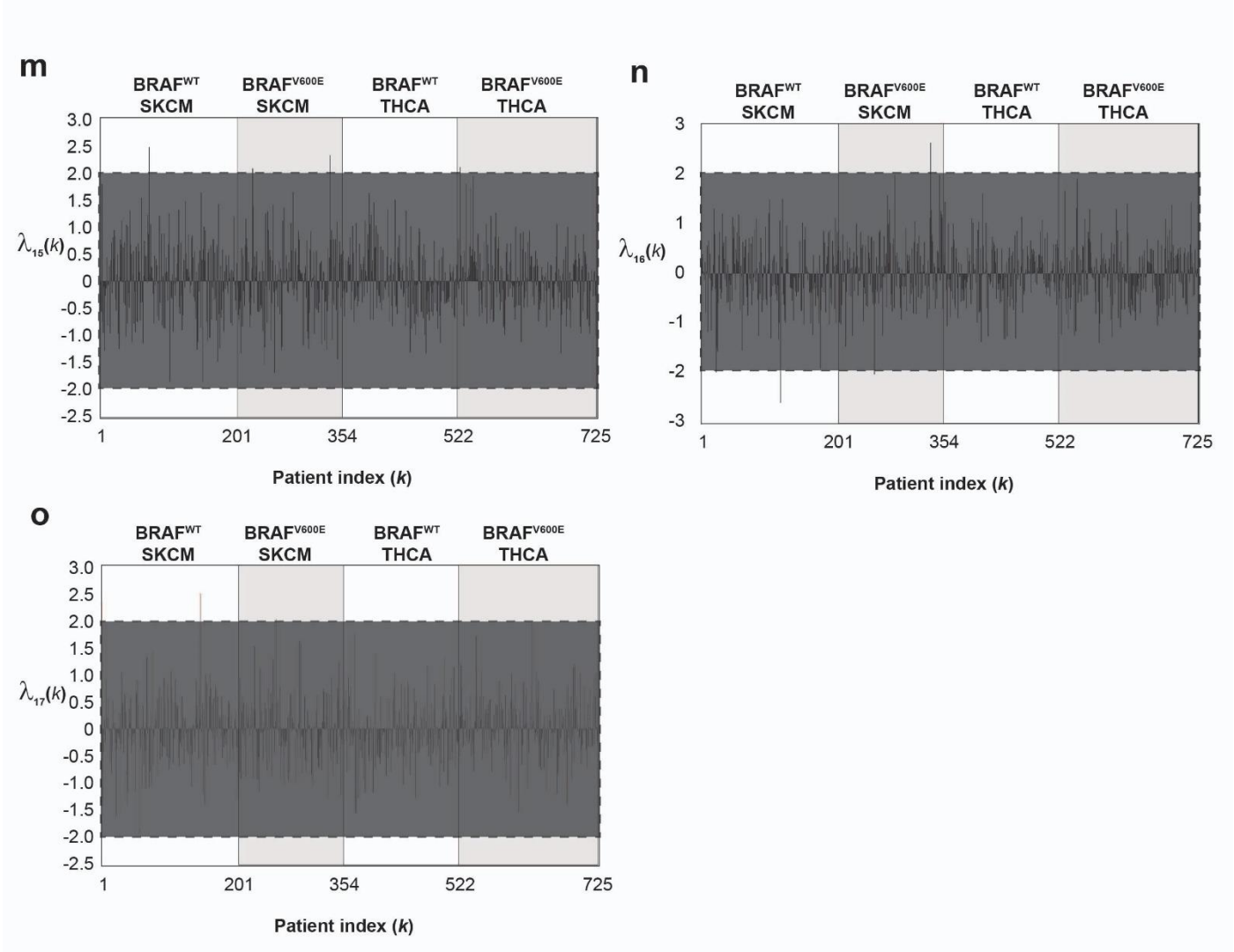


Supplementary Figure 3. Tumor-specific amplitudes (λα(k)) of the 17 unbalanced processes. Not all unbalanced processes are active in all patients. Rather, each unbalanced process, α, is assigned an amplitude, λα(k), for the specific tumor, k (see also Supplementary Data 1). Every panel in the figure presents 725 values of λα(k) for a specific value of α. The gray boxes mark the threshold limits – only values greater than 2 or smaller than -2 were considered significant (see Methods for more details).

**Supplementary Figure 4.**

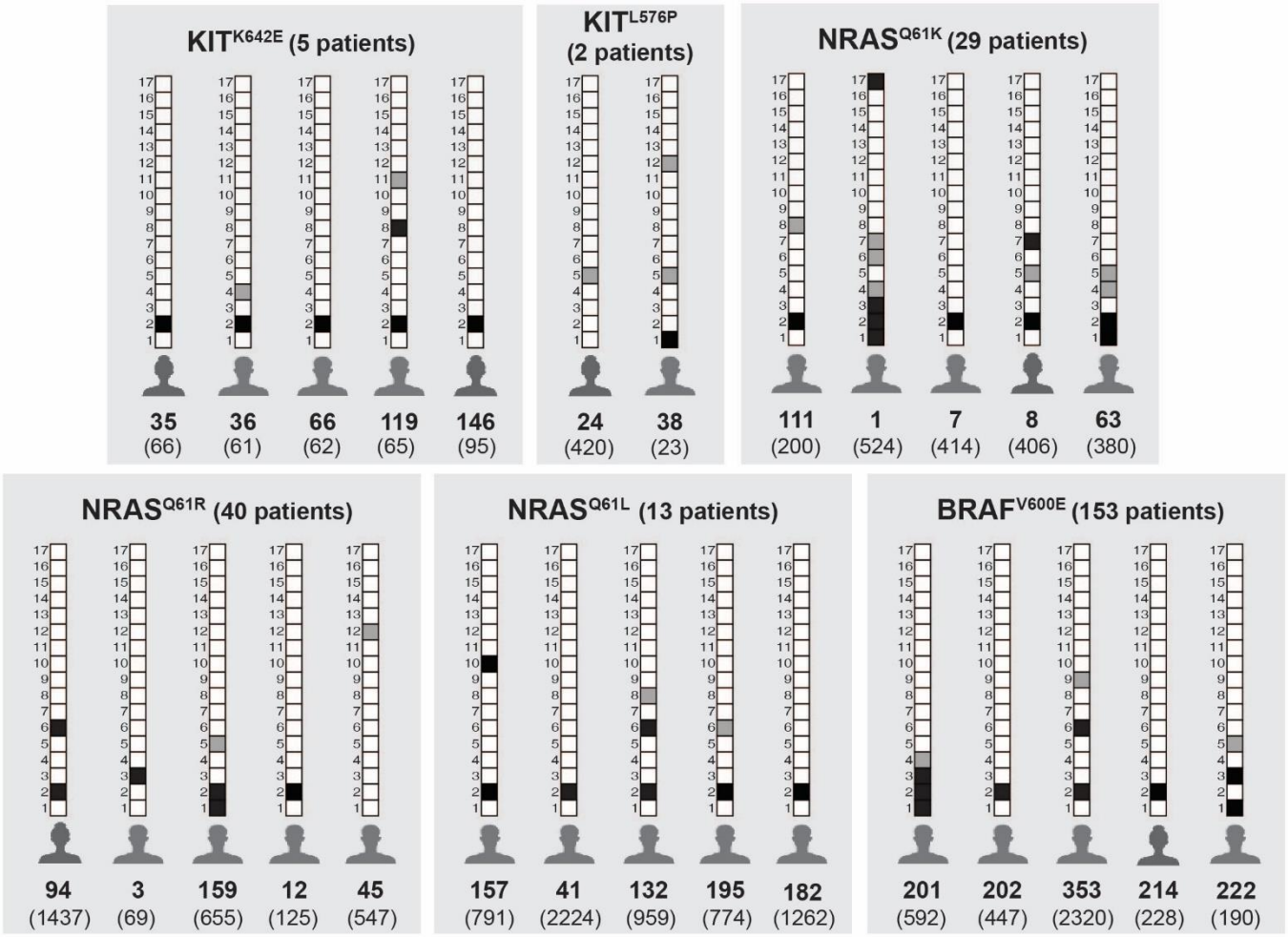


**Supplementary Figure 4. SKCM patients harboring the same genomic mutations are characterized by various PaSSS-based barcodes.** Patient-specific data regarding common mutations in melanoma was obtained from the GDC Data Portal. The full list can be found in Supplementary Data 6. For each mutation, the number of total patients harboring this mutation is stated. The mutations shown are mutually exclusive, namely a patient that harbors one of the mutations does not harbor any of the others [1]. Up to 5 patients were randomly selected for each mutation, and their PaSSS-based barcodes are shown, demonstrating that even though they carry the same mutation, their barcodes of unbalanced processes differ, and may thus demand distinct modes of treatment. The number in brackets (under patient index) denotes the total number of mutations, according to patient-specific data from cBioportal.org.

**Supplementary Figure 5.**

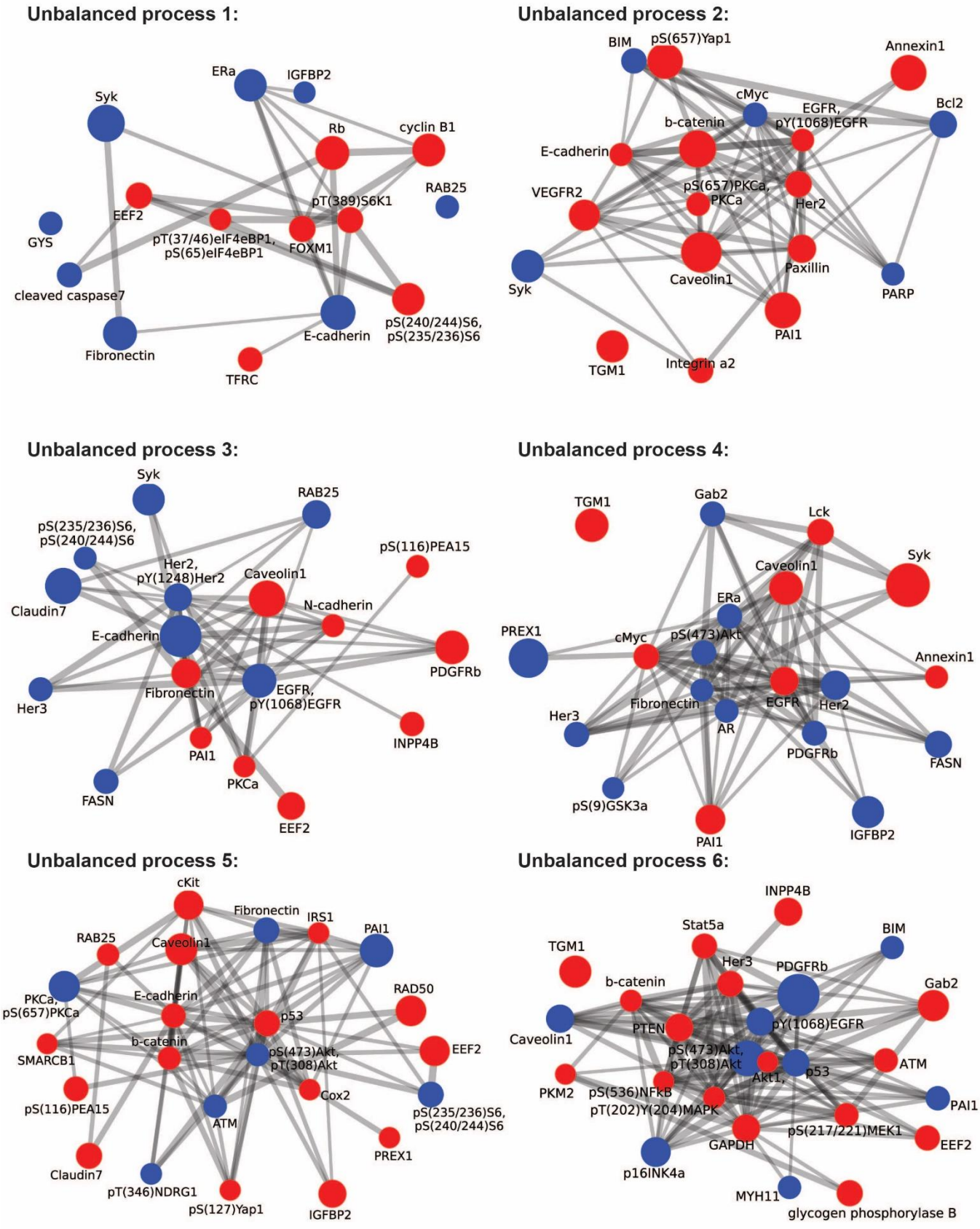

**Unbalanced process 7:**

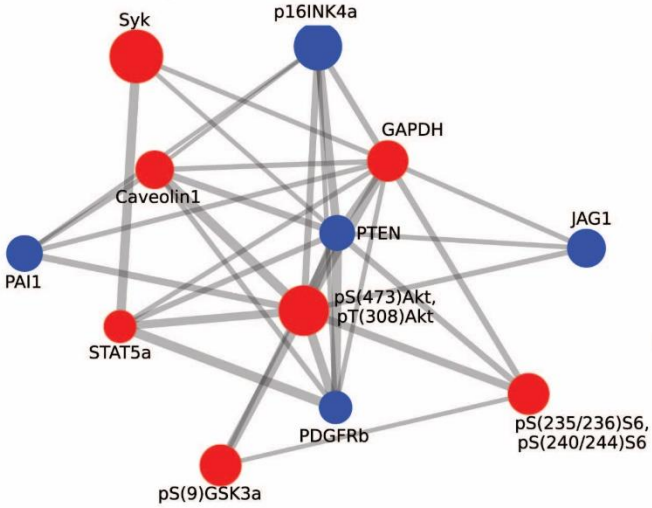


**Unbalanced process 8:**

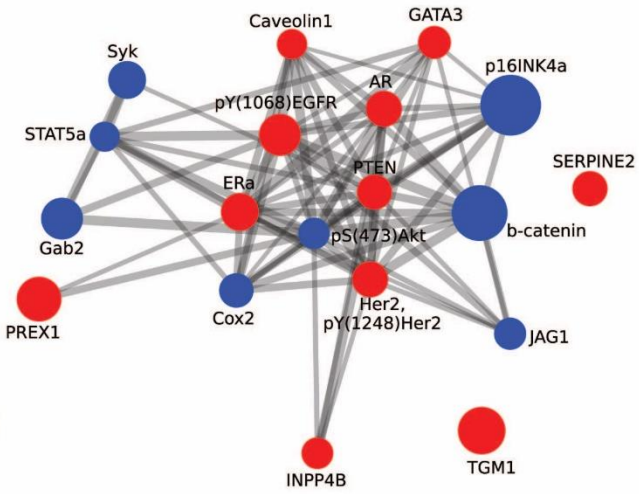


**Unbalanced process 9:**

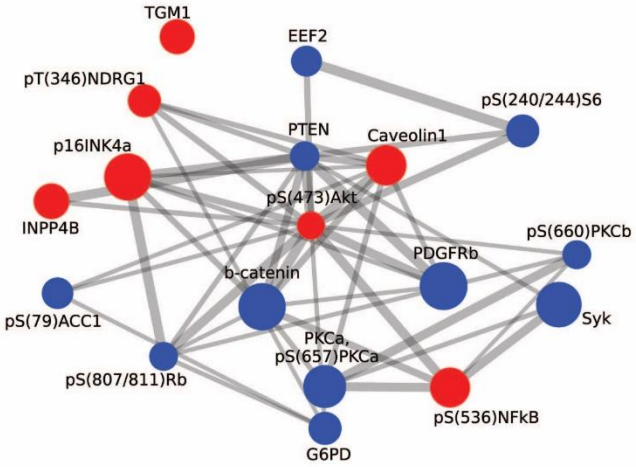


**Unbalanced process 10:**

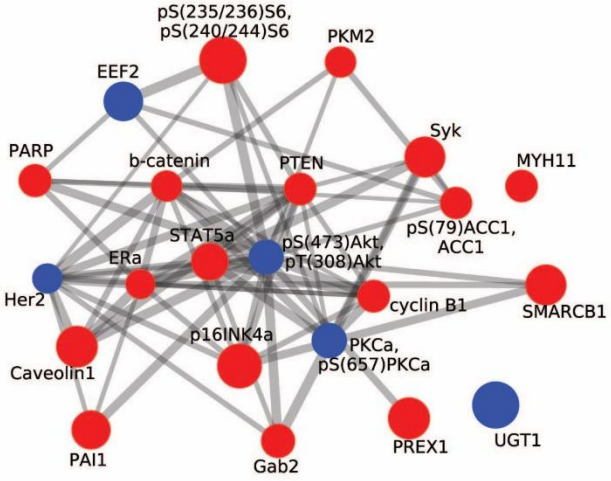


**Unbalanced process 11:**

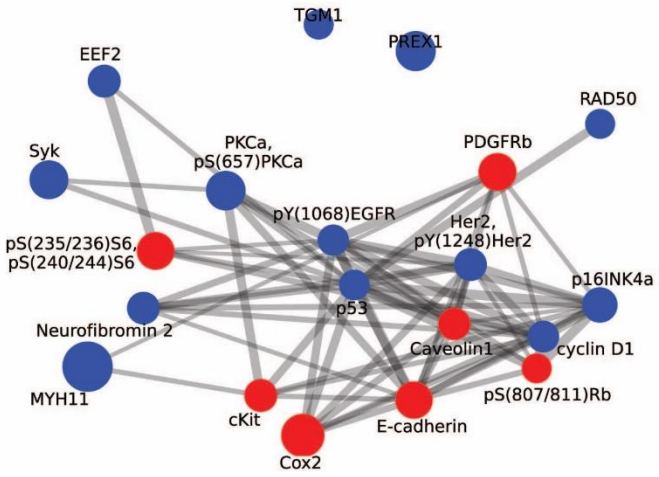


**Unbalanced process 12:**

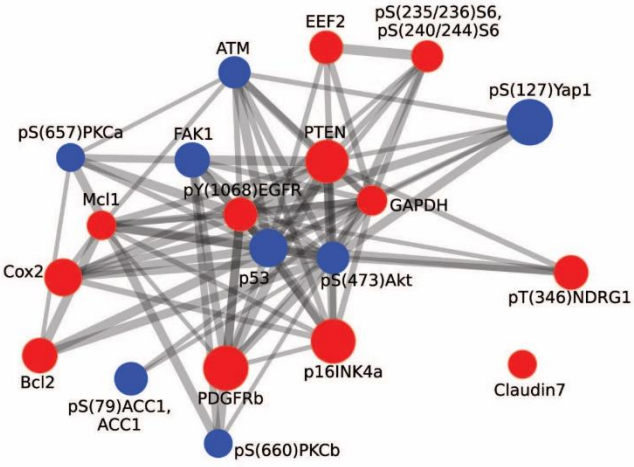

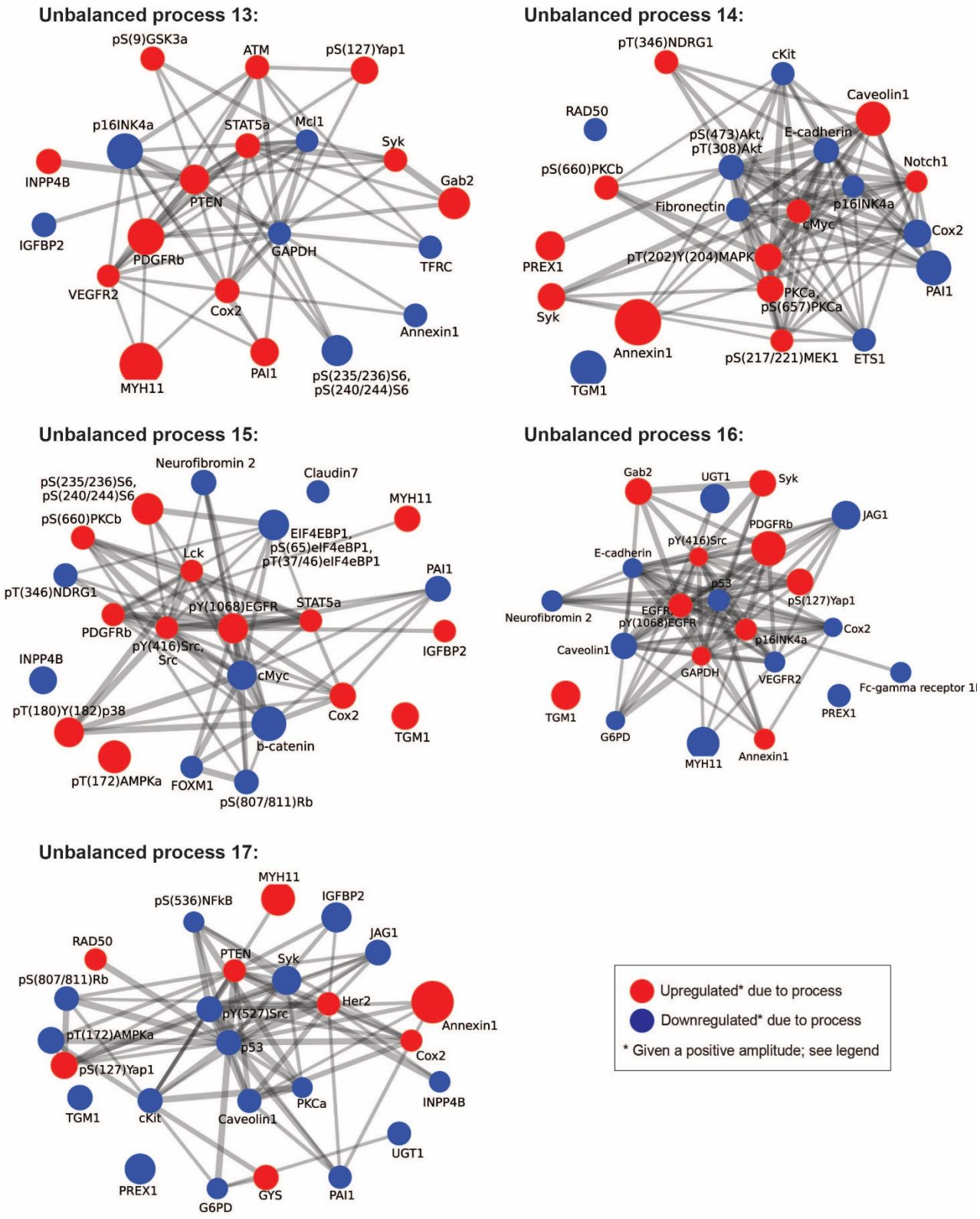


**Supplementary Figure 5. The unbalanced subnetworks identified by PaSSS analysis for 219 cell lines.** For every process α, the proteins were assembled into networks using functional interactions according to STRING database. **Note** that red proteins are upregulated, and blue proteins are downregulated given that the amplitude of the process is positive. In tumors where the amplitude is negative, the direction of change is opposite.

**Supplementary Figure 6.**

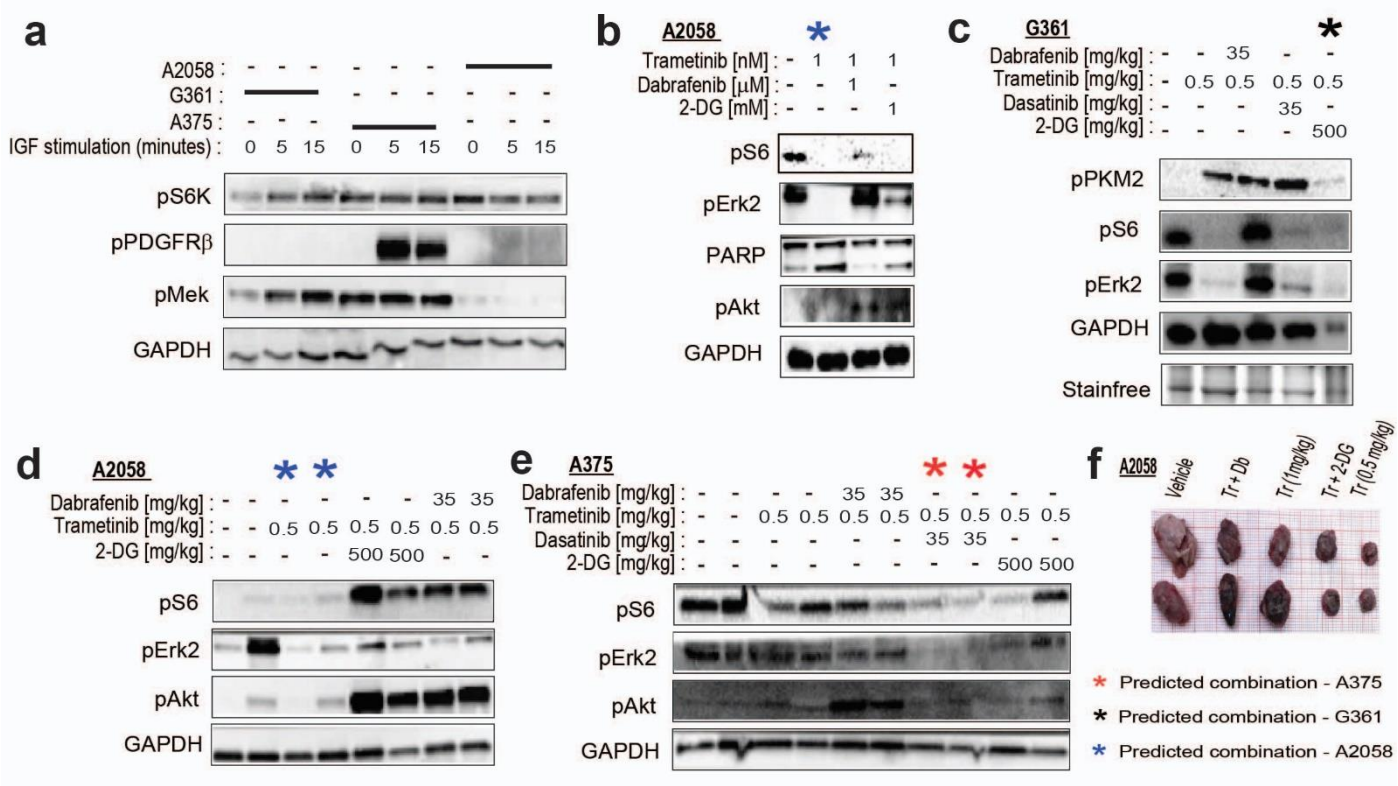


**Supplementary Figure 6: Comparison of 3 BRAF-mutated melanoma malignancies and their altered signaling signatures in vitro and in vivo. (a)** Western blot results comparing the basal state of 3 melanoma malignancies upon stimulation with IGF at different time points. The central druggable targets representing the PaSSS of each cell line are shown. pS6K (representative of unbalanced process 1) is expressed in all 3 cell lines. pPDGFR (representative of unbalanced process 3) is active only in A375 as suggested by the analysis, whereas pMEK (representative of unbalanced process 6) is active in A375 and G361. (**b**) Western blot results of A2058 following treatment with different therapies *in vitro*. The predicted therapy depletes the signaling in A2058 cells as represented by the decrease in phosphorylation levels of pS6 and pERK. (**c**) Western blot results of G361 tumors following treatment with different therapies *in vivo*. To show a long-term effect of the combined treatment on GAPDH levels, western blot analysis was performed on tissues harvested following 25 days of treatment. The predicted combination depletes the signaling in G361 tumors, as represented by the decrease in phosphorylation levels of pS6, pPKM2 and pERK. (**d**) Western blot results of A2058 tumors following treatment with different therapies *in vivo*. The predicted therapy depletes the signaling in A2058 tumors as represented by the decrease in phosphorylation levels of pAKT and pERK. (**e**) Western blot results of A375 tumors following treatment with different therapies *in vivo*. The effect of the predicted combinations on phospho-levels (d,e) was examined 7 days following the beginning of the treatment. (**f**) The size of A2058 tumors following treatment with different therapies. Lower concentrations of trametinib were more efficient in inhibiting tumor growth than higher concentrations.

**Supplementary Figure 7.**

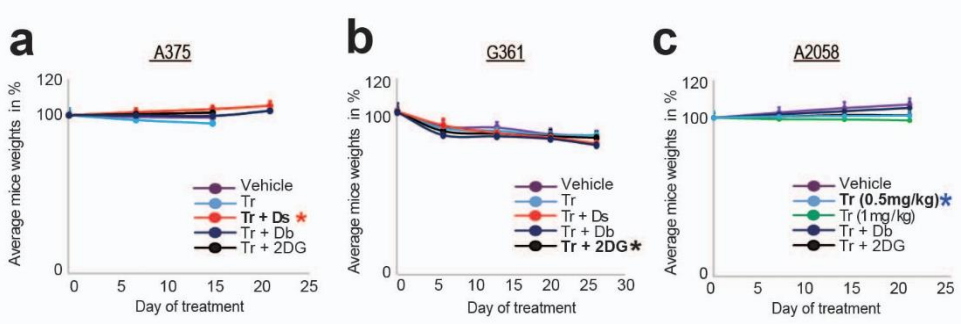


**Supplementary Figure 7: Mice treated with SA-based drug combinations demonstrated no significant weight loss *in vivo*.** A375 (**a**), G361 (**b**) or A2058 (**c**) were injected subcutaneously into mice, and once tumors reached 50 $mm^3$, treatments were initiated. In all three cases, the PaSSS-based drug combinations or the monotherapy of trametinib or the combinations predicted to partially target the PaSSS did not cause any significant weight loss in the mice (less than 12% from the start of treatment) during the course of the treatment.

## Supplementary Data Legends

Supplementary Data 1-9 are provided as excel files.

Each Supplementary Data file includes a legend located in the first tab of the dataset. The legend provides full description of the content.

# Original Western Blots

**Original blots for Figure 5:**

pS6

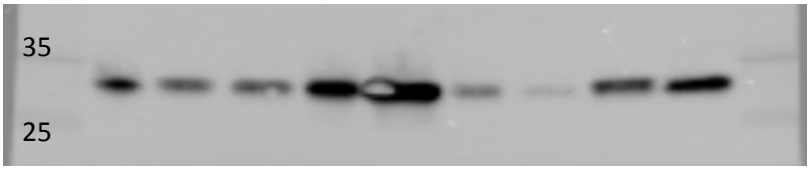


pErk2

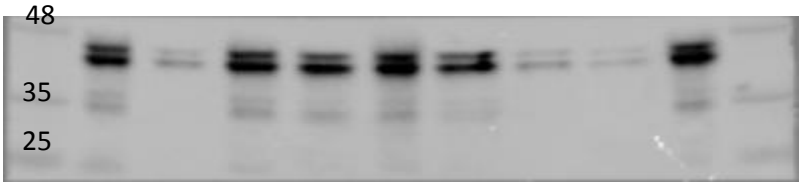


pAkt

pPDGFRb

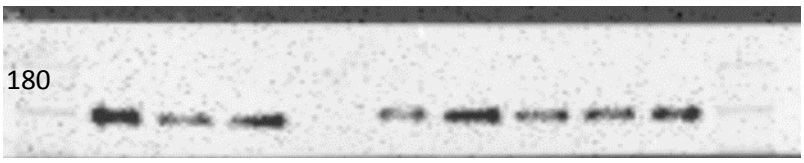


pPKM2

P53

PARP

PS6K

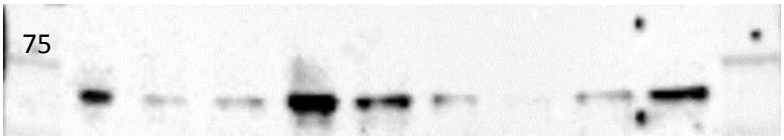


GAPDH

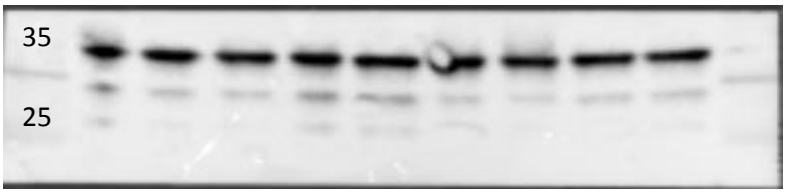


**Original blots for Figure 6:**

pS6

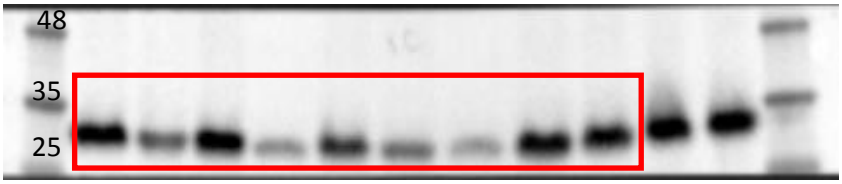


pERK2

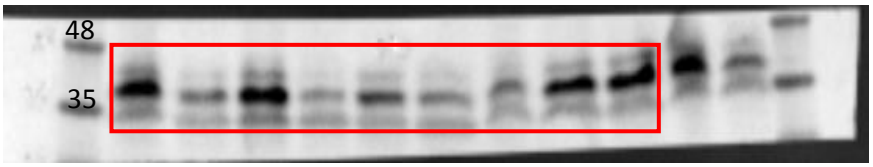


pAkt

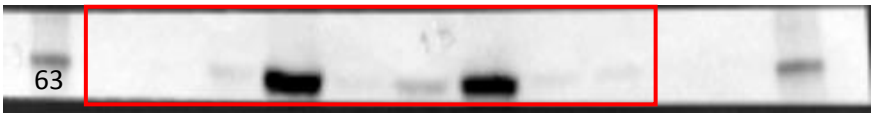


GAPDH

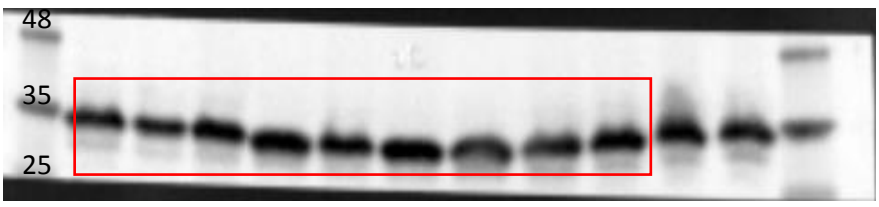

pPKM2

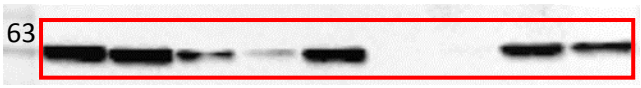


PS6K

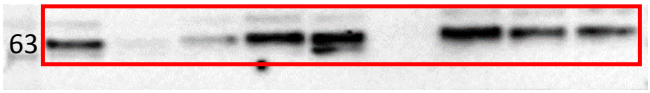


**Original blots for Supplementary Figure 6a:**

PS6K

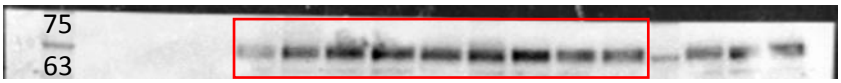


pPDGFRb

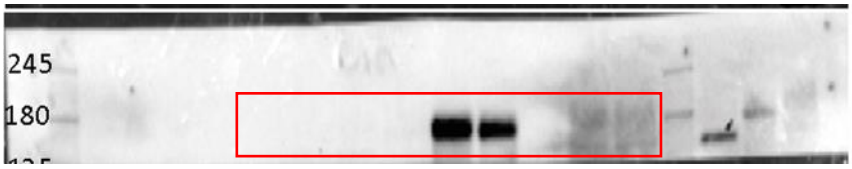


pMEK

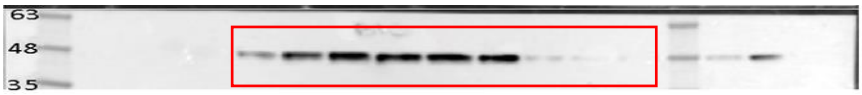


GAPDH

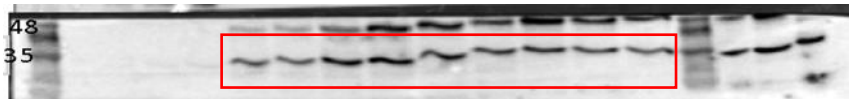

**Original blots for Supplementary Figure 6b:**

pS6

pERK

PARP

pAKT

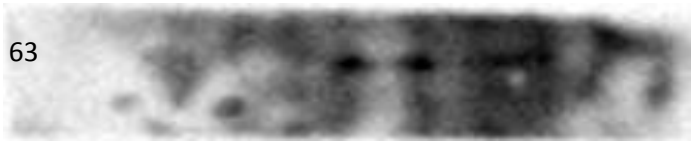


GAPDH

**Original blots for Supplementary Figure 6c:**

pPKM2

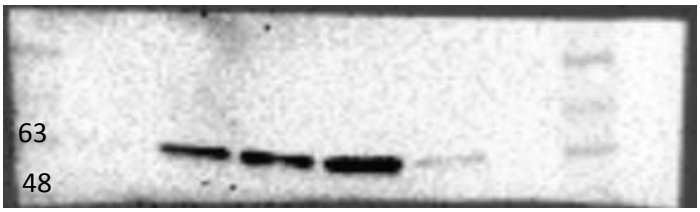


pS6

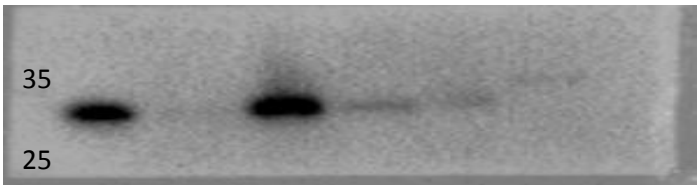


pErk

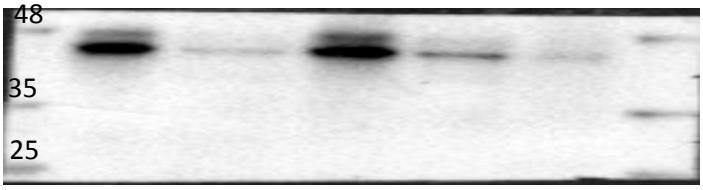


GAPDH

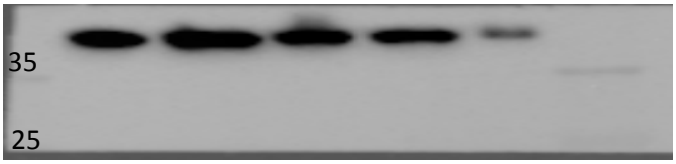

**Original blots for Supplementary Figure 6d:**

pS6

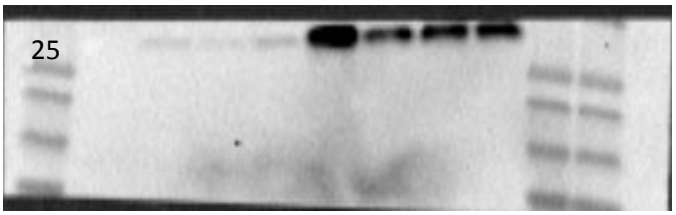


pERK2

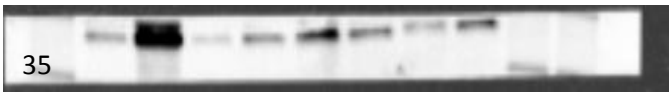


pAkt

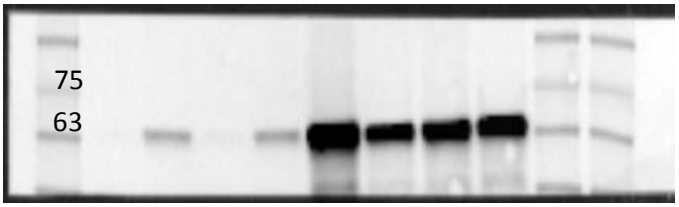


GAPDH

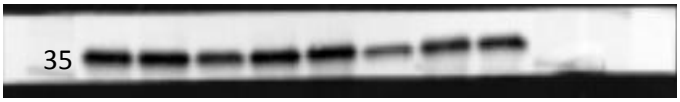

**Original blots for Supplementary Figure 6e:**

pS6

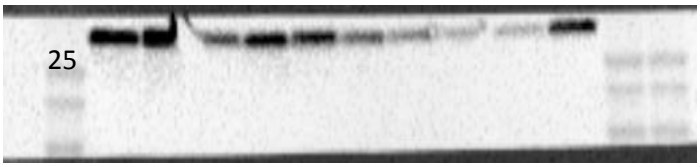


pErk2

pAkt

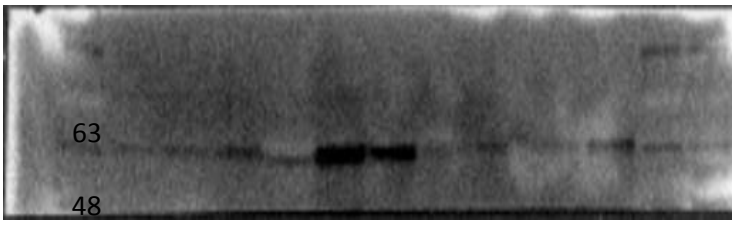


GAPDH

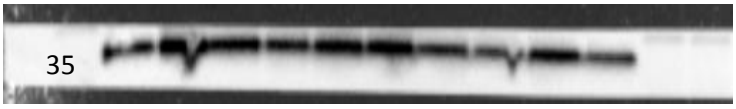

## Supplementary References

1. Luo C, Shen J. Research progress in advanced melanoma. Vol. 397, Cancer Letters. Elsevier Ireland Ltd; 2017. p. 120–6.